Electronic Supplementary Material (ESI) for Physical Chemistry Chemical Physics.

Supplementary information for

Alleviating stability-performance contradiction of cage-like high-energy-density-materials by backbone-collapse and branch-heterolysis competition mechanism

Qingguan Song,[a,b,c] *Lei Zhang,*[a,b]* *and Zeyao Mo* [a,b]*

[a]*Institute of Applied Physics and Computational Mathematics, Beijing, 100088, China*

[b]*CAEP Software Center for High Performance Numerical Simulation, Beijing, 100088, China*

[c]*Institute of Chemical Materials, China Academy of Engineering Physics, Mianyang, 621999, China*

† Correspondence: Lei Zhang (zhang_lei@iapcm.ac.cn) and Zeyao Mo (zeyao_mo@iapcm.ac.cn)

Calculation method of detonation performance parameters

The detonation performance parameters of HEDMs were calculated at the crystal level. The maximum heat of explosion Q_{max} was determined by the energy difference between the total energy of the unreacted crystal and the total energy of all detonation products. Wherein the distribution of the detonation products is determined based on the principle of minimization of their Gibbs free energy. Once the Q_{max} is known, the detonation velocity D and the detonation pressure $P_{C\text{-}J}$ can be derived from the Kamlet-Jacobs formula:

$$D = 1.01\left(N^{\frac{1}{2}} M^{\frac{1}{4}} \left(Q_{\max}\right)^{\frac{1}{4}} \right)\left(1+1.3\rho\right)$$

$$P_{C-J} = 1.588\rho^2 N M^{\frac{1}{2}} \left(Q_{\max}\right)^{\frac{1}{2}}$$

Wherein N is the number of moles of gaseous detonation products per gram of explosive, M is the average molecular weight of these gases, and ρ is the density. For more details, please turn to our previous work[1-3].

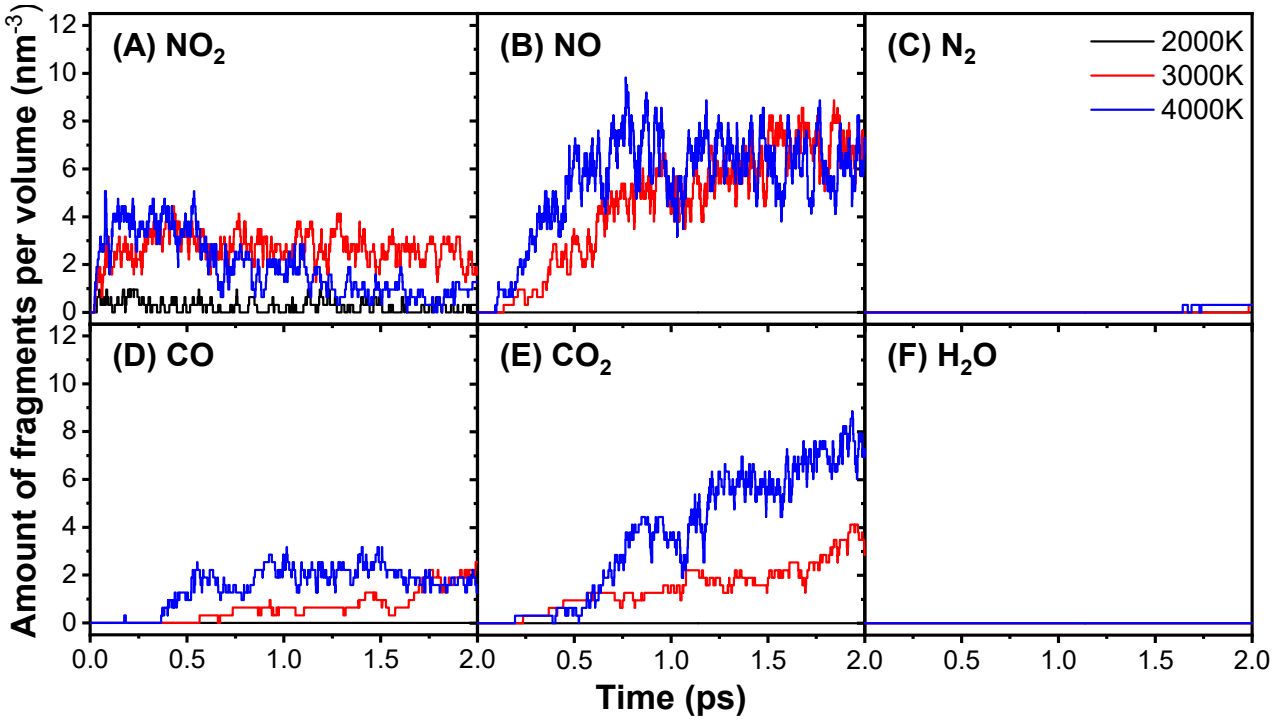

Figure S1 Amount of generated intermediate fragments as a function of time during the quantum mechanical molecular dynamics simulation of early thermolysis of ONC at the temperatures of 2000, 3000, and 4000 K.

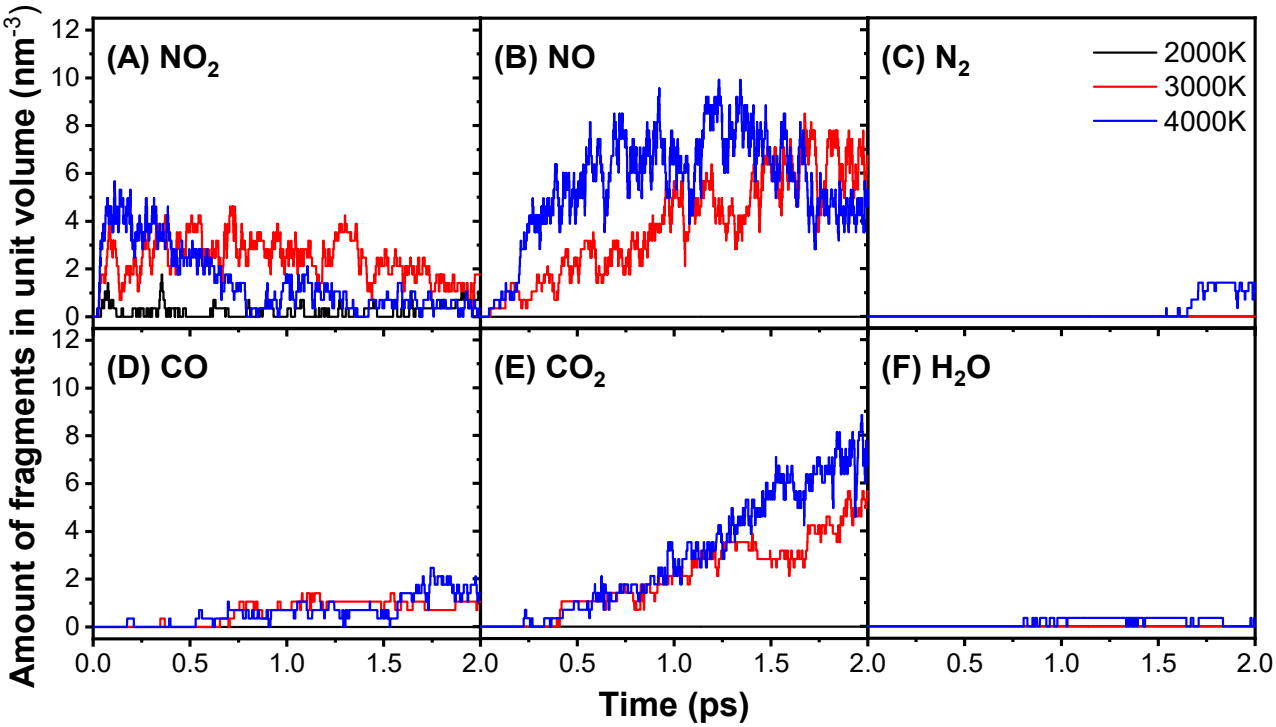

Figure S2 Amount of generated intermediate fragments as a function of time during the quantum mechanical molecular dynamics simulation of early thermolysis of HNC at the temperatures of 2000, 3000, and 4000 K.

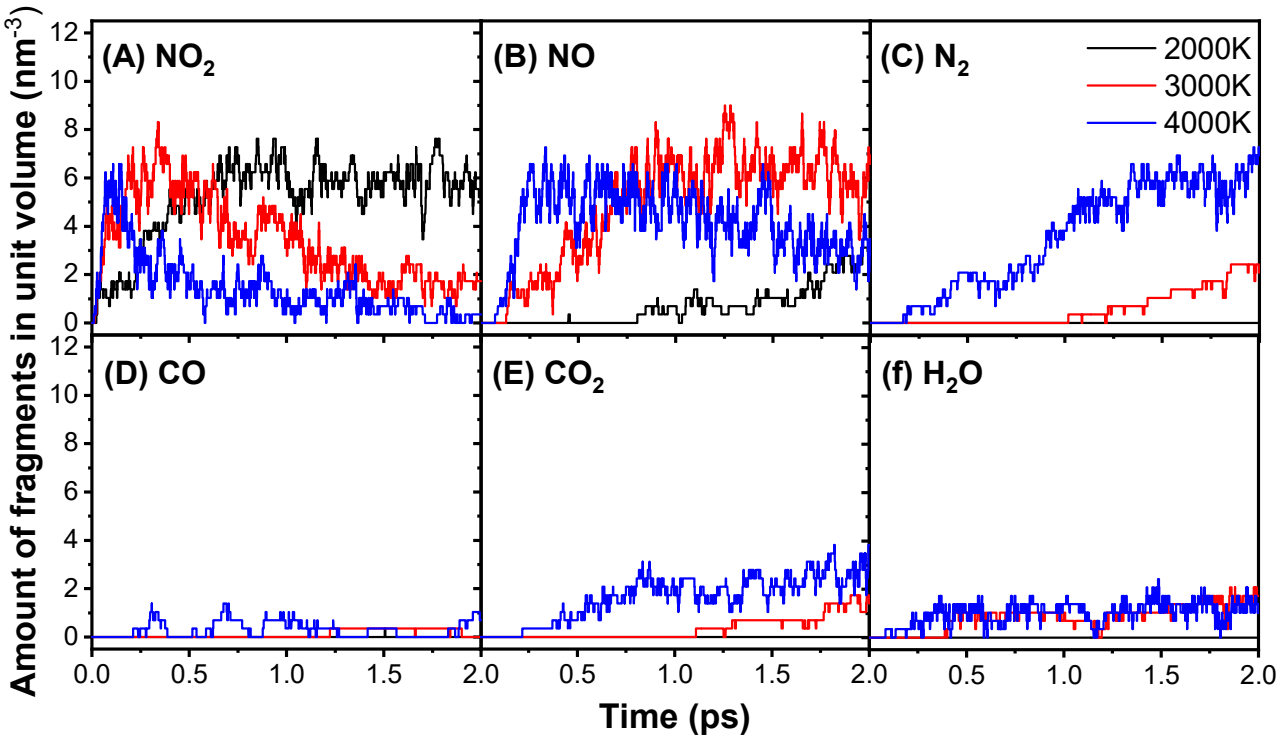

Figure S3 Amount of generated intermediate fragments as a function of time during the quantum mechanical molecular dynamics simulation of early thermolysis of CL-20 at the temperatures of 2000, 3000, and 4000 K.

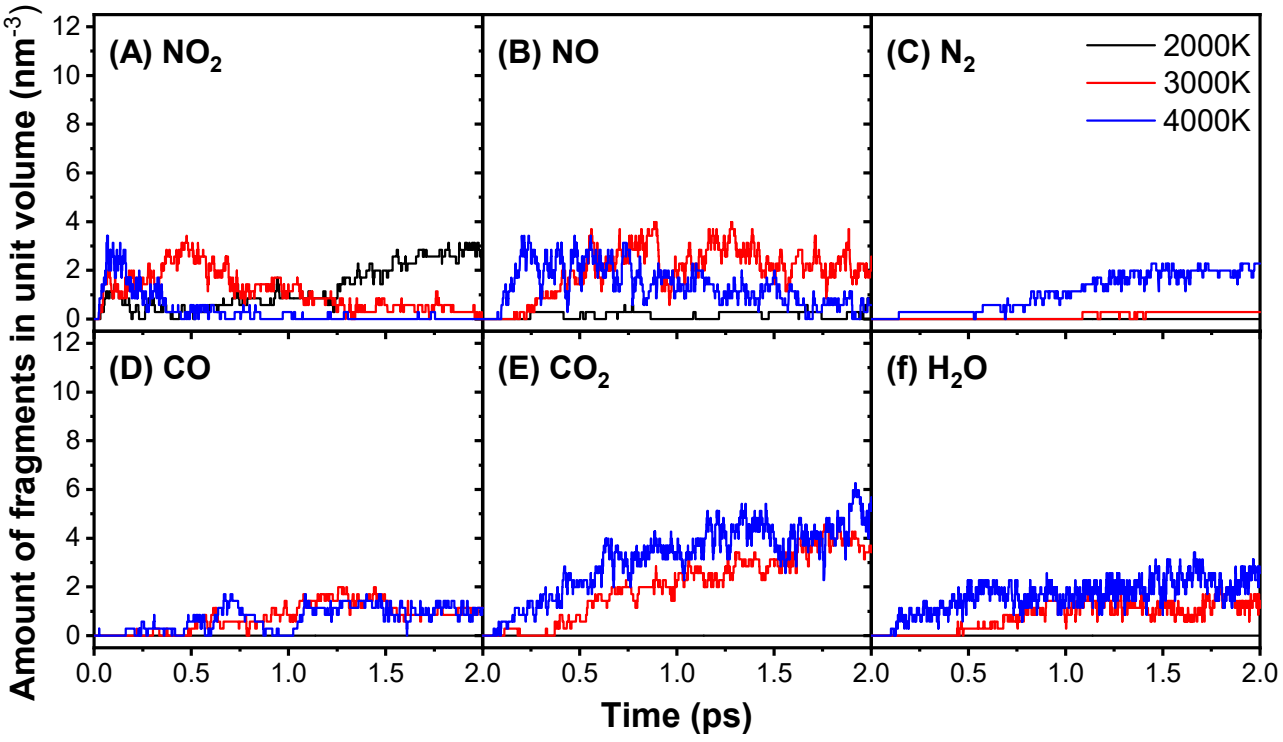

Figure S4 Amount of generated intermediate fragments as a function of time during the quantum mechanical molecular dynamics simulation of early thermolysis of TEX at the temperatures of 2000, 3000, and 4000 K.

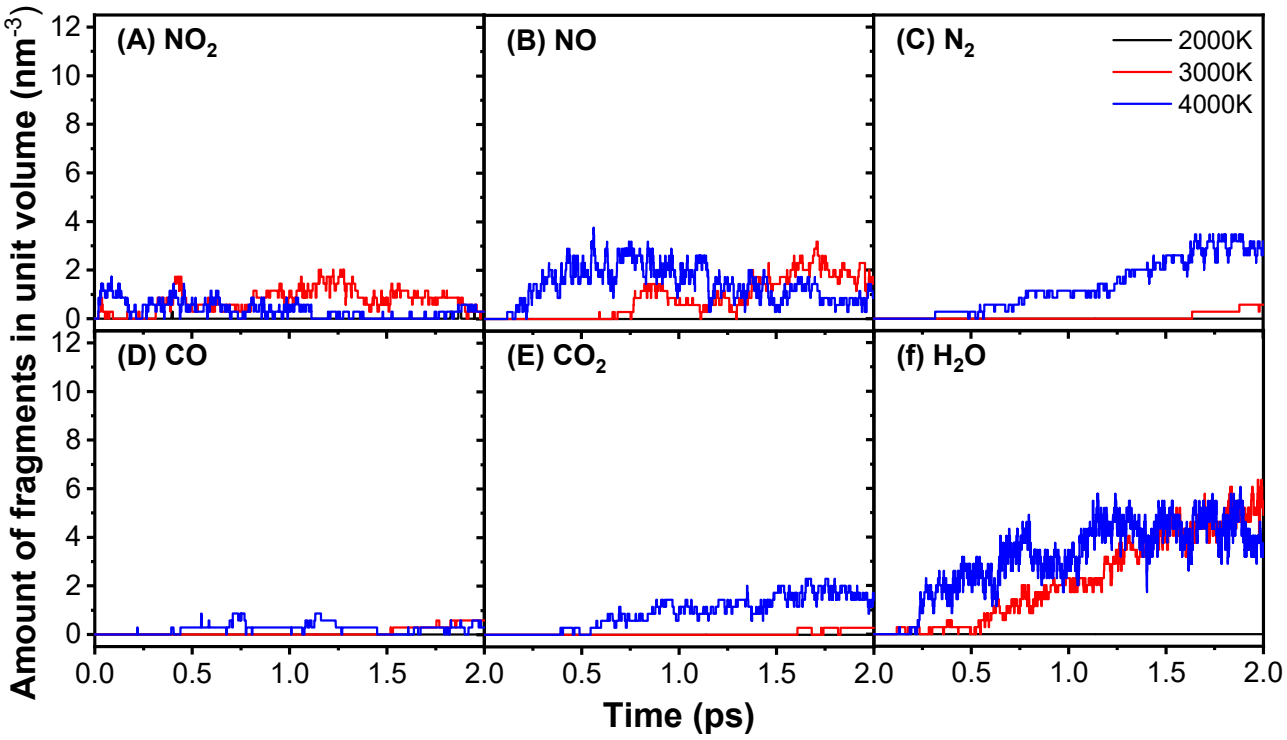

Figure S5 Amount of generated intermediate fragments as a function of time during the quantum mechanical molecular dynamics simulation of early thermolysis of TATB at the temperatures of 2000, 3000, and 4000 K.

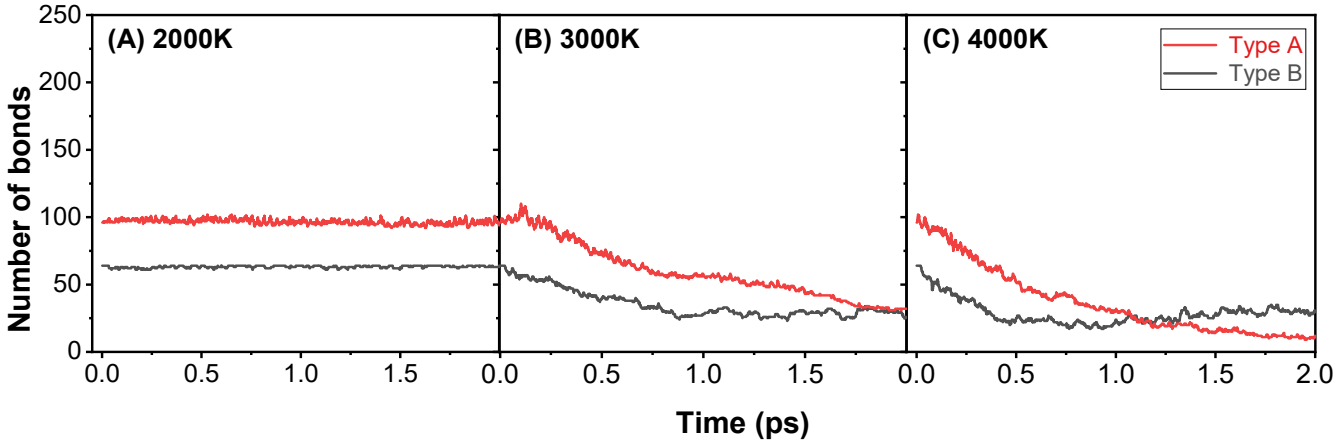

Figure S6 Number of two types of chemical bonds as a function of simulation time for ONC thermolysis at temperatures of (A) 2000 K, (B) 3000 K, and (C) 4000 K. Type A represents for backbone connection, and type B is branch connection.

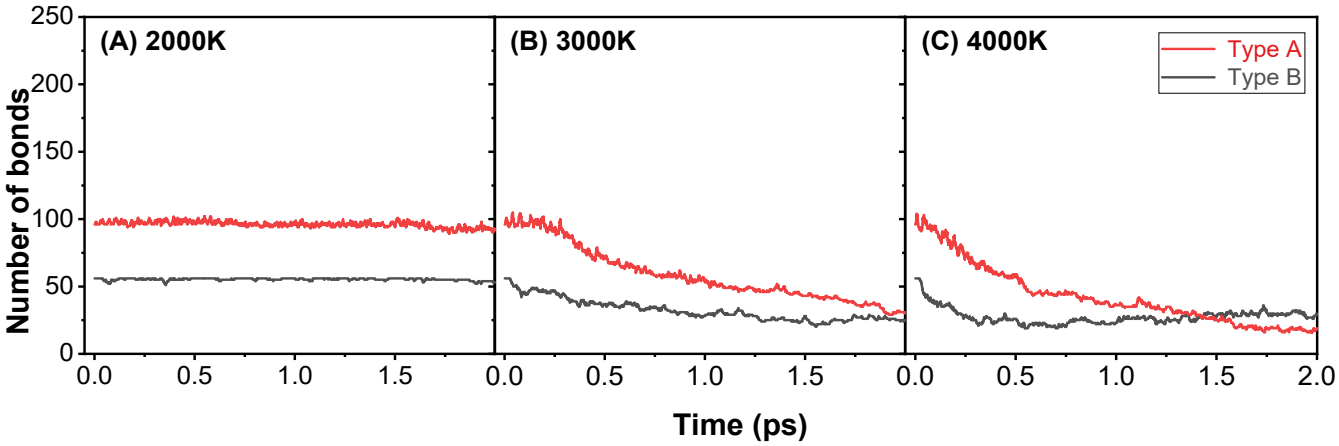

Figure S7 Number of two types of chemical bonds as a function of simulation time for HNC thermolysis at temperatures of (A) 2000 K, (B) 3000 K, and (C) 4000 K. Type A represents for backbone connection, and type B is branch connection.

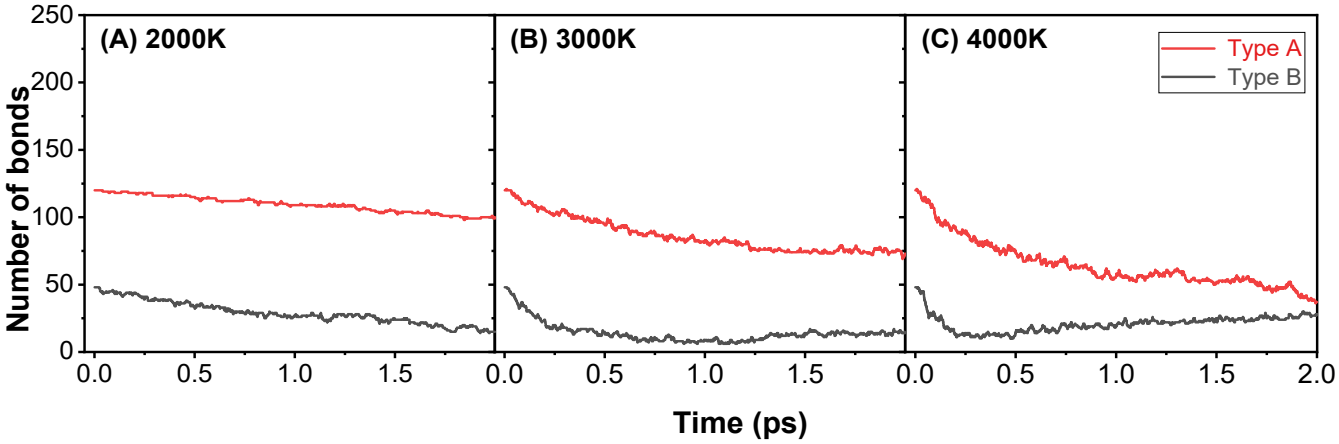

Figure S8 Number of two types of chemical bonds as a function of simulation time for CL-20 thermolysis at temperatures of (A) 2000 K, (B) 3000 K, and (C) 4000 K. Type A represents for backbone connection, and type B is branch connection.

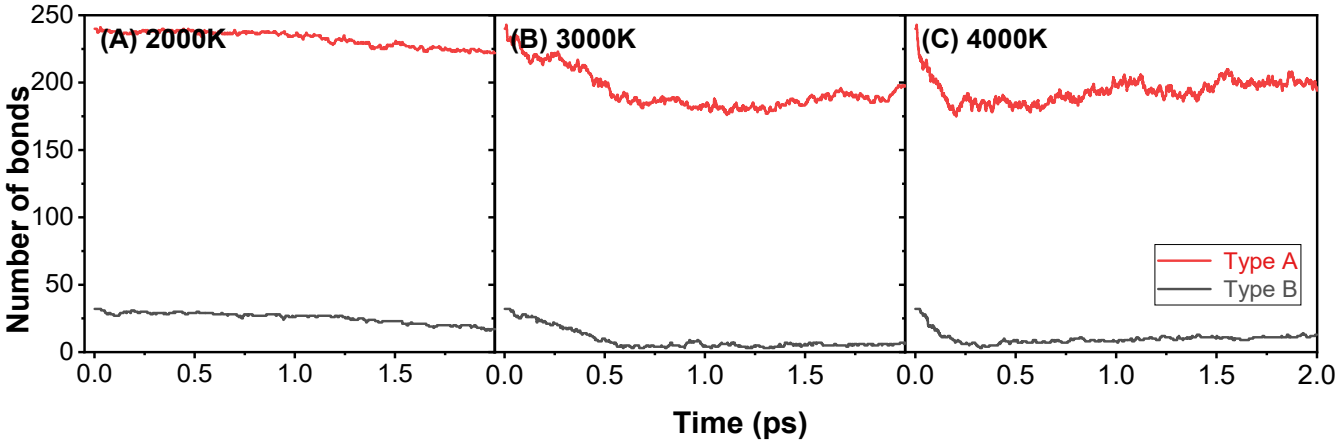

Figure S9 Number of two types of chemical bonds as a function of simulation time for TEX thermolysis at temperatures of (A) 2000 K, (B) 3000 K, and (C) 4000 K. Type A represents for backbone connection, and type B is branch connection.

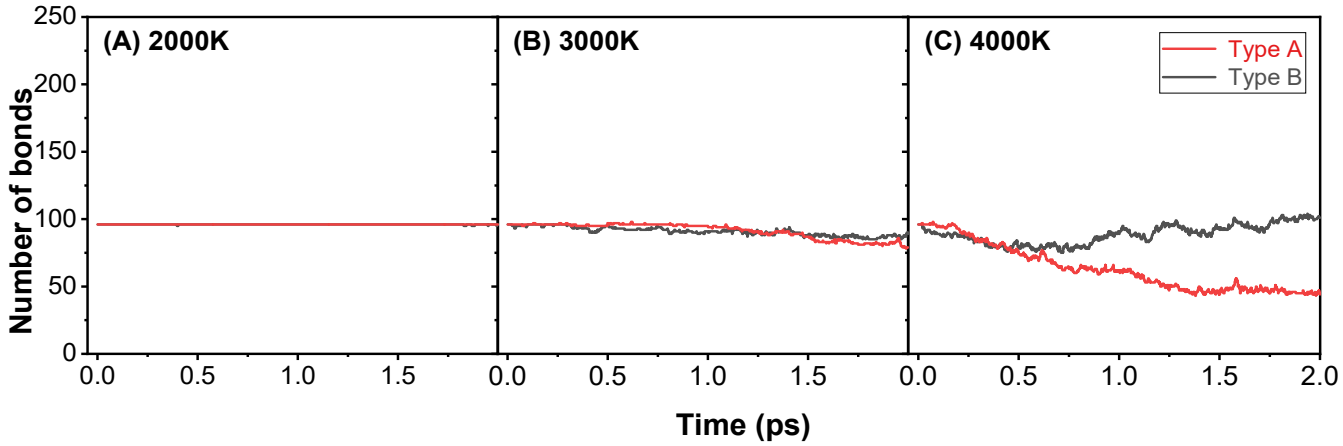

Figure S10 Number of two types of chemical bonds as a function of simulation time for TATB thermolysis at temperatures of (A) 2000 K, (B) 3000 K, and (C) 4000 K. Type A represents for backbone connection, and type B is branch connection.

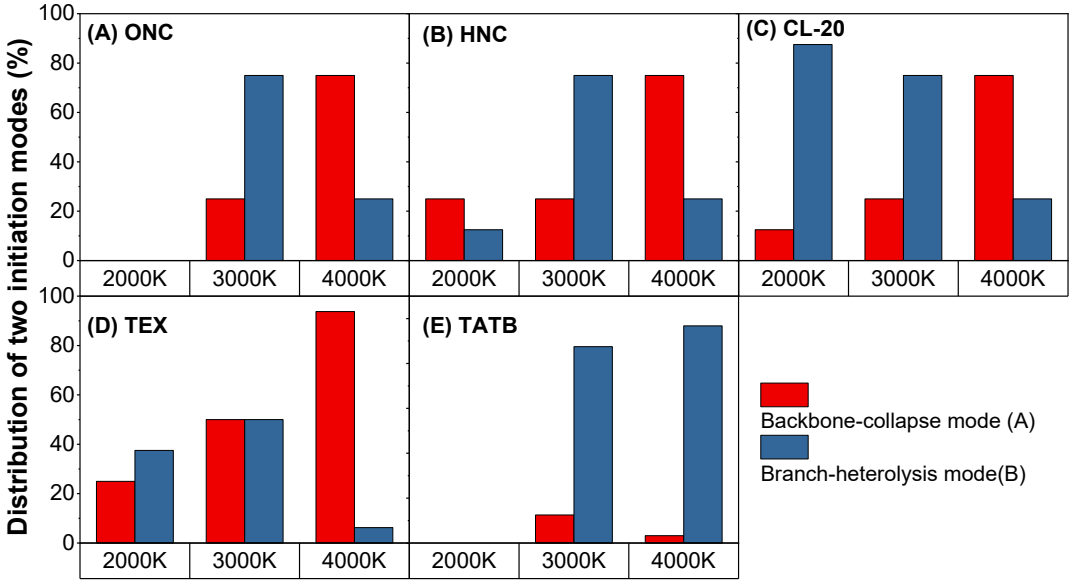

Figure S11 Distribution of backbone-collapse and branch-heterolysis modes in thermolysis initiation of the HEDMs studied.

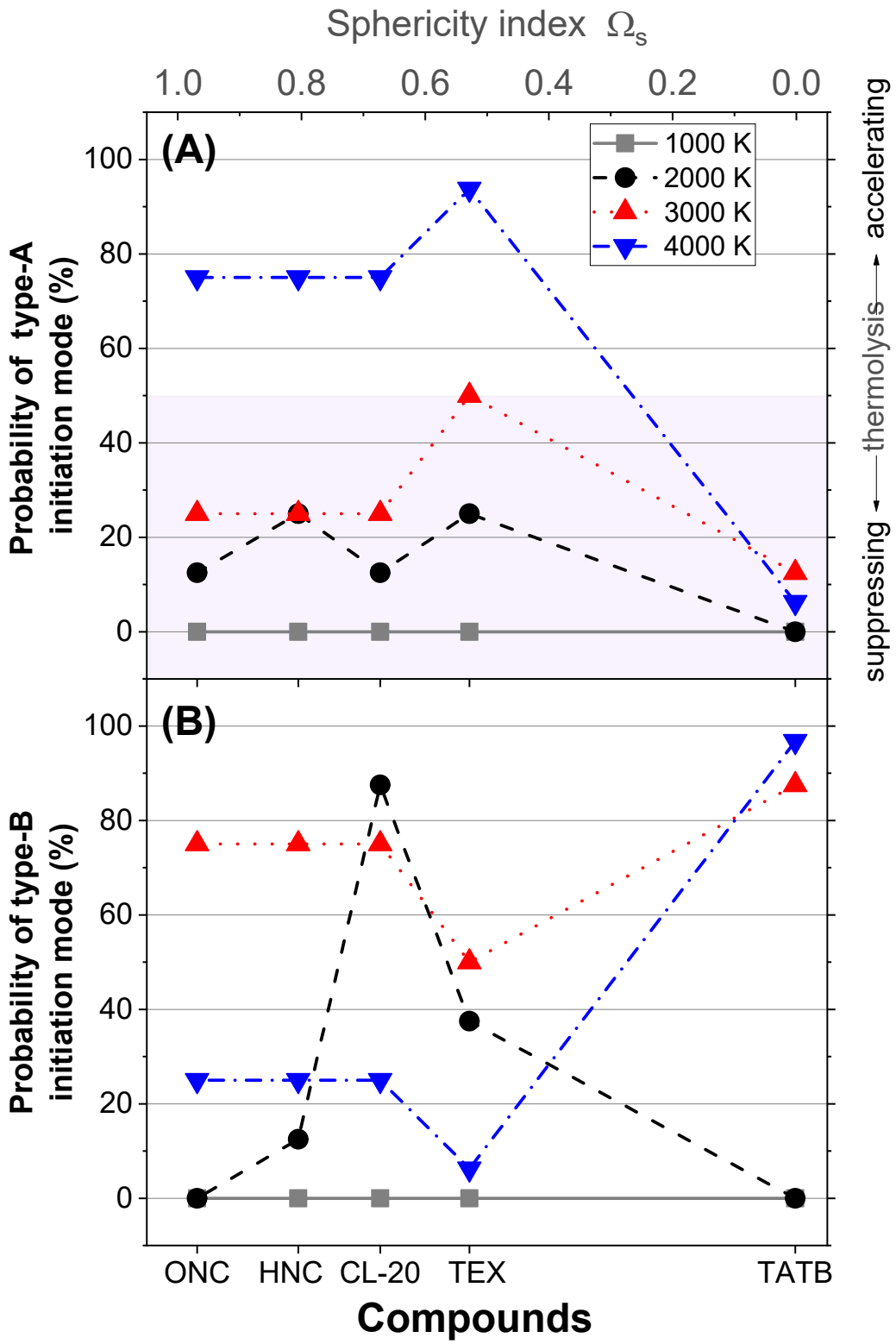

Figure S12 Distribution of backbone-collapse and branch-heterolysis modes in thermolysis initiation of the HEDMs studied. The probabilities of the two initialization modes are plotted with (A, C) increasing temperature, and (B, D) decreasing spherical index, respectively.

Table S1 Calculated lattice vector lengths [Å], angles [º], and volumes [Å^3] of the primitive cells of ONC, HNC, CL-20, TEX, and TATB, along with experimental results in the literature.

Compounds	Method	*a*	*b*	*c*	*α*	*β*	*γ*	Volume
ONC	This work	12.91	8.93	20.27	90.00	137.54	90.00	1577.61
	Expt. [4]	12.79	8.84	20.18	90.00	136.90	90.00	1558.31
	Error	+0.94%	+1.02%	+0.45%	0.00%	+0.47%	0.00%	+1.24%
HNC	This work	23.85	8.16	14.52	90.00	90.00	90.00	2823.24
	Expt. [4]	23.59	8.17	14.26	90.00	90.00	90.00	2750.81
	Error	+1.10%	-0.12%	+1.82%	0.00%	0.00%	0.00%	+2.63%
CL-20	This work	8.92	12.64	13.37	90.00	106.64	90.00	1443.80
	Expt.[5]	8.86	12.59	13.39	90.00	106.92	90.00	1430.24
	Error	+0.68%	+0.40%	-0.15%	0.00%	-0.26%	0.00%	+0.95%
TEX	This work	6.85	7.71	8.82	79.07	74.60	82.57	439.31
	Expt. [6]	6.85	7.66	8.84	79.41	74.89	82.44	438.20
	Error	0.00%	+0.65%	-0.23%	-0.43%	-0.39%	+0.16%	+0.25%
TATB	This work	9.10	9.11	6.47	119.89	91.77	107.73	431.65
	Expt. [6]	9.01	9.03	6.81	119.97	91.82	108.58	442.49
	Error	+0.93%	+0.85%	-4.97%	-0.06%	-0.05%	-0.79%	-2.45%

Table S2 Primitive cell expansions, dimensions, and number of atoms of the constructed supercells of ONC, HNC, CL-20, TEX, and TATB for molecular dynamics simulations of early thermolysis.

Compounds	Expansion	Dimension	Number of atoms
ONC	1×2× 1	12.91 Å × 17.86 Å × 20.27 Å	256
HNC	1×1×1	23.85 Å × 8.16 Å × 14.52 Å	240
CL-20	2×1×1	17.83 Å × 12.64 Å × 13.37 Å	288
TEX	2×2×2	13.69 Å × 15.42 Å × 17.65 Å	384
TATB	2×2×2	18.19 Å × 18.21 Å × 12.95 Å	384

Table S3 Elementary reactions of thermolysis of TATB at temperatures of 1000-4000K.

Temperature	Main reactions	Duration(fs)	Number of occurrences
1000K	No reaction	-	-
2000K	No reaction	-	-
3000K	$C_6H_6O_6N_6 \rightarrow NO_2+C_6H_6O_4N_5$	31.9-949.8	9
	$C_6H_xO_kN_m+C_6H_yO_lN_n \leftrightarrow C_{12}H_{x+y}O_{k+l}N_{m+n}$ $C_{12}H_xO_kN_m+C_6H_yO_lN_n \leftrightarrow C_{18}H_{x+y}O_{k+l}N_{m+n}$	18.4-1087.7	157

	$C_{18}H_xO_kN_m+C_6H_yO_lN_n \leftrightarrow C_{24}H_{x+y}O_{k+l}N_{m+n}$		
	$NO_2+C_6H_xO_kN_m \leftrightarrow C_6H_xO_{k+2}N_{m+1}$	39.0-1067.8	142
	$H+HO \leftrightarrow H_2O$ $H+H_2O \leftrightarrow H_3O$ $NO_2+H \leftrightarrow HONO$	235.1-1994.3	298
4000K	$C_6H_6O_6N_6 \rightarrow NO_2+C_6H_6O_4N_5$	19.6-566.6	5
	$C_6H_xO_kN_m+C_6H_yO_lN_n \leftrightarrow C_{12}H_{x+y}O_{k+l}N_{m+n}$ $C_{12}H_xO_kN_m+C_6H_yO_lN_n \leftrightarrow C_{18}H_{x+y}O_{k+l}N_{m+n}$ $C_{18}H_xO_kN_m+C_6H_yO_lN_n \leftrightarrow C_{24}H_{x+y}O_{k+l}N_{m+n}$ $C_{24}H_xO_kN_m+C_6H_yO_lN_n \leftrightarrow C_{30}H_{x+y}O_{k+l}N_{m+n}$ $C_{30}H_xO_kN_m+C_6H_yO_lN_n \leftrightarrow C_{36}H_{x+y}O_{k+l}N_{m+n}$	18.5-439.7	43
	$NO_2+C_6H_xO_kN_m \leftrightarrow C_6H_xO_{k+2}N_{m+1}$ $H_2O+C_6H_xO_kN_m \leftrightarrow C_6H_{x+2}O_{k+1}N_m$	23.2-584.2	36
	$NO_2+H \leftrightarrow HNO_2$ $H+HO \leftrightarrow H_2O$ $H+CON \leftrightarrow CHON$ $H+H_2O \leftrightarrow H_3O$	33.4-1996.0	1024

Table S4 Calculated detonation performance parameters of the five HEDMs studied, including detonation velocity (D), detonation pressure ($P_{C\text{-}J}$), and heat of explosion (Q_{max}). Available experimental data searched from references were presented for comparison.

Explosive	Method	D (km/s)	$P_{C\text{-}J}$ (GPa)	Q_{max} (kJ/g)
ONC	This work	9.56	43.61	7.97
	Exp.	9.80 [7]	44.92 [8]	-
	Error	2.50%	2.90%	-
HNC	This work	9.39	42.06	7.83
	Exp.	-	-	-
	Error	-	-	-
CL-20	This work	9.30	41.76	5.91
	Exp.	9.40 [9]	42.00 [7]	6.08 [10]
	Error	1.00%	0.60%	2.90%
TEX	This work	8.21	32.20	4.63
	Exp.	8.18 [11]	32.25 [12]	-
	Error	0.30%	0.20%	-
TATB	This work	7.68	28.17	3.72
	Exp.	7.76 [13]	26.88 [14]	3.91[15]
	Error	1.04%	4.80%	4.86%

References:

1. Zhang, L.; Wu, J. Z.; Jiang, S. L.; Yu, Y.; Chen, J., From Intermolecular Interactions to Structures and Properties of a Novel Cocrystal Explosive: A First-Principles Study. *Phys Chem Chem Phys* **2016**, *18*, 26960-26969.
2. Li, C.; Li, H.; Zong, H.; Huang, Y.; Gozin, M.; Sun, C.; Zhang, L., Strategies for Achieving Balance between Detonation Performance and Crystal Stability of High-Energy-Density Materials. *iScience* **2020**, *23*, 100944.
3. Huang, X.; Li, C.; Tan, K.; Wen, Y.; Guo, F.; Li, M.; Huang, Y.; Sun, C.; Gozin, M.; Zhang, L., Applying Machine Learning to Balance Performance and Stability of High Energy Density Materials. *iScience* **2021**, *24*, 102240.
4. Zhang, M. X.; Eaton, P. E.; Gilardi, R., Hepta- and Octanitrocubanes. *Angew. Chem. Int. Ed.* **2000**, *39*, 401.
5. Bolotina, N. B.; Hardie, M. J.; Speer Jr, R. L.; Pinkerton, A. A., Energetic Materials: Variable-Temperature Crystal Structures of Γ- and ∈-Hniw Polymorphs. *J. Appl. Crystallogr.* **2004**, *37*, 808-814.
6. Gatilov, Y. V.; Rybalova, T. V.; Efimov, O. A.; Lobanova, A. A.; Sakovich, G. V.; Sysolyatin, S. V., Molecular and Crystal Structure of Polycyclic Nitramines. *Journal of Structural Chemistry* **2005**, *46*, 566-571.
7. Talawar, M. B.; Sivabalan, R.; Mukundan, T.; Muthurajan, H.; Sikder, A. K.; Gandhe, B. R.; Rao, A. S., Environmentally Compatible Next Generation Green Energetic Materials (Gems). *J. Hazard Mater.* **2009**, *161*, 589-607.
8. Liu, M. H.; Lin, C. C., Theoretical Modeling of the Chemical Synthesis and Detonation Performance of Polynitrocubane Derivatives. *International Journal of Quantum Chemistry* **2019**, *120*.
9. Venugopalan, S., *Demystifying Explosives*; Demystifying Explosives: Pune, 2015.
10. Agrawal, J. P., *High Energy Materials-Propellants, Explosives and Pyrotechnics*; Wiley-VCH: Weinheim, 2010.
11. RudolfMeyer; JosefKöhler; Homburg, A., *Explosives*; WileyVCH: Weinheim, 2015.
12. Türker, L.; Variş, S., On the Possibility of Autoxidation of Tex - a Dft Study. *Propell. Explos. Pyrot.* **2015**, *40*, 81-87.
13. Keshavarz, M. H., Estimating Heats of Detonation and Detonation Velocities of Aromatic Energetic Compounds. *Propellants, Explosives, Pyrotechnics* **2008**, *33*, 448-453.
14. Wang, G.; Xiao, H.; Ju, X.; Gong, X., Calculation of Detonation Velocity, Pressure, and Electric Sensitivity of Nitro Arenes Based on Quantum Chemistry. *Propellants, Explosives, Pyrotechnics* **2006**, *31*, 361-368.
15. Akst, I. B., Heat of Detonation, the Cylinder Test, and Performance Munitions. **1989**.